

Sigmoidal crack growth rate curve: statistical modelling and applications

Original

Sigmoidal crack growth rate curve: statistical modelling and applications / Paolino, D.S., Cavatorta, M.P.. - In: FATIGUE & FRACTURE OF ENGINEERING MATERIALS & STRUCTURES. - ISSN 8756-758X. - STAMPA. - 36:4(2013), pp. 316-326. [10.1111/ffe.12001]

Availability:

This version is available at: 11583/2502668 since:

Publisher:

Wiley-Blackwell

Published

DOI:10.1111/ffe.12001

Terms of use:

This article is made available under terms and conditions as specified in the corresponding bibliographic description in the repository

Publisher copyright

(Article begins on next page)

Please cite this article as:

“PAOLINO, D.S. and CAVATORTA, M.P., 2013. Sigmoidal crack growth rate curve: Statistical modelling and applications. *Fatigue and Fracture of Engineering Materials and Structures*, **36**(4), pp. 316-326.”

Sigmoidal crack-growth-rate curve: statistical modeling and applications

Authors:

D.S. Paolino^a, M.P. Cavatorta^b

^a Department of Mechanical and Aerospace Engineering, Politecnico di Torino, 10129 Turin, Italy,
davide.paolino@polito.it

^b Department of Mechanical and Aerospace Engineering, Politecnico di Torino, 10129 Turin, Italy,
maria.cavatorta@polito.it

Corresponding Author:

D.S. Paolino

E-mail address: davide.paolino@polito.it

Full postal address:

C.so Duca degli Abruzzi 24,

Department of Mechanical and Aerospace Engineering – Politecnico di Torino,
10129 – Torino,

ITALY

Phone number: +39.011.090.5746

Fax number: +39.011.090.6999

Abstract:

The present paper proposes a statistical model for describing sigmoidal crack growth rate curves. Major novelties are: a) exploitation of the Maximum Likelihood Principle for obtaining material estimates by pooling together experimental data belonging to the different crack propagation regions; b) a general formulation which allows to adopt different sigmoidal models and any kind of statistical distribution for the model variables; c) fatigue life predictions through numerical integration of analytical functions with no need of Monte Carlo simulations.

Experimental data taken from NASGRO database are used to check the validity of the statistical model in estimating material parameters included in the crack growth NASGRO algorithm. Illustrative plots of number of cycles to failure and crack length after a given number of cycles are presented, showing good agreement between the proposed statistical model and NASGRO results.

Keywords:

Fatigue crack growth; NASGRO; probabilistic model; life prediction; crack length prediction

Nomenclature

a = crack length

$a_0, A_0, A_k, B_k, C_{th}^-, C_{th}^+, p, q, t_0, \rho_S$ = constant coefficients of NASGRO model

a_c = critical crack length

$a_{c,\gamma}, a_{e_{a_s,N},\gamma}, N_{f_{a_s},\gamma}, v_{a,1-\gamma}, \tilde{v}_{a,\gamma}^*$ = γ -th or $(1 - \gamma)$ -th quantiles

$a_{e_{a_s,N}}$ = final crack length after N cycles

a_s = initial crack length

C, n = random coefficients of NASGRO model

$E[\cdot]$ = expectation of a random variable

f, k_1, k_2 = functions in NASGRO model

$f_{K_c}, f_{K_{Ic}}, f_{v_a}, f_{v_a|(\Delta K_{th}, K_c)}, f_{v_a|(\Delta K_{th1,\infty}, K_{Ic})}, f_{\Delta K_{th}}, f_{\Delta K_{th1,\infty}}$ = probability density functions

$F_{a_c}, F_{a_{e_{a_s,N}}}, F_{N_{f_{a_s}}}, F_{K_c}, F_{v_a|(\Delta K_{th}, K_c)}, F_{v_a}, F_{\Delta K_{th}}$ = cumulative distribution functions

K_c = fracture toughness

K_{Ic} = plane strain fracture toughness

$K_c^*, K_{Ic}^*, v_a^*, \Delta K_{th}^*, \Delta K_{th1,\infty}^*$ = values assumed by random variables

$\underline{K_c^*}, K_{Ic,min}, \underline{\Delta K_{th}^*}, \Delta K_{th1,\infty,min}$ = lower limits of integration

$\overline{K_c^*}, K_{Ic,max}, \overline{\Delta K_{th}^*}, \Delta K_{th1,\infty,max}$ = upper limits of integration

K_{max} = maximum stress intensity factor (SIF)

K_{min} = minimum SIF

L = Likelihood function

N = number of cycles

$N_{f_{a_s}}$ = number of cycles to failure

$P[\cdot]$ = probability of an event

R = stress ratio

S_y = yield strength

t = thickness

$v_a = \ln[da/dN]$ = natural logarithm of the crack growth rate

Y = geometry factor for SIF computation

ΔK = SIF range

ΔK_{th} = random threshold SIF range

$\Delta K_{th1,\infty}$ = random threshold SIF range at $R \rightarrow 1$ and for long cracks ($a \gg a_0$)

$\Delta \sigma$ = stress range

$\mu_C, \mu_{K_{Ic}}, \mu_n, \mu_{v_a}, \mu_{\Delta K_{th1,\infty}}$ = location parameters

ρ = correlation coefficient between C and n

$\sigma_C, \sigma_{K_{Ic}}, \sigma_n, \sigma_{v_a}, \sigma_{\Delta K_{th1,\infty}}$ = scale parameters

$\phi[\cdot]$ = standardized Normal probability density function

$\Phi[\cdot]$ = standardized Normal cumulative distribution function

$\theta = (\theta_1, \theta_2, \dots, \theta_r)$ = set of parameters in Likelihood function

$\tilde{\cdot}$ = estimate

$\cdot | \cdot$ = conditional event

1. Introduction

Fatigue crack growth is statistical in nature. Life prediction and reliability evaluation are critical for the design and maintenance planning of many structural components. Different algorithms for predicting life of cracked components are available in the literature. However, as well discussed in¹, most algorithms are not able to take into account statistical variability of the many material parameters that are necessary to describe the crack growth phenomenon.

In general, crack propagation curves are represented in the double logarithmic plot of crack growth rate, da/dN , versus the stress intensity factor (SIF) range, ΔK . Curves show a typical sigmoidal shape with three distinct crack propagation regions: (I) near-threshold region limited by threshold stress intensity factor range, ΔK_{th} ; (II) stable crack propagation region described by the well-known Paris power law; (III) unstable crack propagation region controlled by fracture toughness, K_c .

Starting from Paris law, different models have been proposed to include the near-threshold region and, in fewer cases, the unstable crack propagation region (e.g., Collipriest², Priddle³, NASGRO⁴). These models, all deterministic in nature, describe the sigmoidal shape of the empirical crack growth curve. Among these models, due to its completeness, NASGRO algorithm is often considered as the reference algorithm⁵⁻⁷.

Several papers deal with statistical and stochastic models for crack propagation⁸⁻¹⁰. Nevertheless, due to the complexity of the phenomenon, most models¹¹⁻¹⁶ are only based on the Paris law, so that it is difficult to make a comprehensive evaluation of scatter characteristics of sigmoidal crack growth curves. In more recent works^{1,5,7,17,18} a nonlinear fitting is applied to experimental data in the attempt to model the whole sigmoidal shape. Data fitting is applied separately to the different crack propagation regions. When computed, fatigue life predictions employ time intensive Monte Carlo simulations.

In the present paper, a general formulation for the statistical distribution of the crack growth rate is proposed. The formulation allows for: a) exploiting the good asymptotic properties of the Maximum Likelihood (ML) Principle in estimating material parameters by pooling together experimental data points belonging to the three crack propagation regions; b) adopting different sigmoidal models and any kind of statistical distribution for the model variables; c) making fatigue life predictions through numerical integration of analytical functions.

Numerical examples based on NASGRO algorithm illustrate the potentiality of the proposed statistical model.

2. Statistical distribution of crack growth rate

To identify a statistical model for sigmoidal crack-growth-rate curves, some initial hypotheses are required:

- 1) ΔK_{th} is a random variable (rv) with cumulative distribution function (cdf) $F_{\Delta K_{th}}[\cdot]$ and probability distribution function (pdf) $f_{\Delta K_{th}}[\cdot]$: ΔK_{th} values vary randomly from specimen to specimen, even if specimens are made of the same nominal material;
- 2) K_c is a rv with cdf $F_{K_c}[\cdot]$ and pdf $f_{K_c}[\cdot]$: K_c values vary randomly from specimen to specimen, even if specimens are made of the same nominal material;
- 3) ΔK_{th} and K_c are independent rv's;
- 4) the logarithm of the crack growth rate, given that $\Delta K_{th} = \Delta K_{th}^*$ and $K_c = K_c^*$, is a conditional rv, $v_a | (\Delta K_{th}, K_c)$, with cdf $F_{v_a | (\Delta K_{th}, K_c)}[\cdot]$ and pdf $f_{v_a | (\Delta K_{th}, K_c)}[\cdot]$.

Considering hypotheses 1)-2), the probability of having no crack propagation at given minimum SIF, K_{min} , and maximum SIF, K_{max} , is equal to:

$$P[\text{no crack propagation}] = P[\Delta K_{th} \geq (K_{max} - K_{min}), K_c > K_{max}]. \quad (1)$$

Recalling the definition of SIF range, $\Delta K = K_{max} - K_{min}$, and of stress ratio, $R = K_{min}/K_{max} = 1 - \Delta K/K_{max}$, and by taking into account hypothesis 3), Equation (1) becomes:

$$P[\text{no crack propagation}] = (1 - F_{\Delta K_{th}}[\Delta K]) \cdot \left(1 - F_{K_c} \left[\frac{\Delta K}{1-R} \right]\right). \quad (2)$$

It must be pointed out that, for some combinations of ΔK and R values, if ΔK_{th} and K_c are continuous rv's defined on the whole positive real axis, there is a nonzero probability of having a specimen with ΔK_{th} larger than ΔK (meaning no crack propagation) and K_c smaller than K_{max} (meaning specimen failure). This is obviously not acceptable from a physical point of view, since it would mean that specimen failure is admissible in a no crack propagation region. Thus, a fifth hypothesis must be added:

- 5) the event $\Delta K_{th} \leq K_c(1 - R)$ is almost sure (i.e., $P[\Delta K_{th} \leq K_c(1 - R)] = 1$) for any R value smaller than 1.

It is worth noting that hypothesis 5) adds a constraint to the relationship between the distributions of ΔK_{th} and K_c but it is not in contrast with hypothesis 3). Indeed, in order to fulfill hypothesis 5), it is sufficient to assume for ΔK_{th} a continuous distribution with a fixed upper limit value, $\overline{\Delta K_{th}^*}$, and for K_c a continuous distribution with a fixed lower limit value, $\underline{K_c^*}$, larger than $\overline{\Delta K_{th}^*}/(1 - R)$. Once the range of validity of the two distributions has been defined, random values for ΔK_{th} and K_c can be independently drawn, thus fulfilling hypothesis 3).

As shown in Figure 1, hypothesis 5) can be graphically visualized with a ΔK axis representation pertaining to a single specimen.

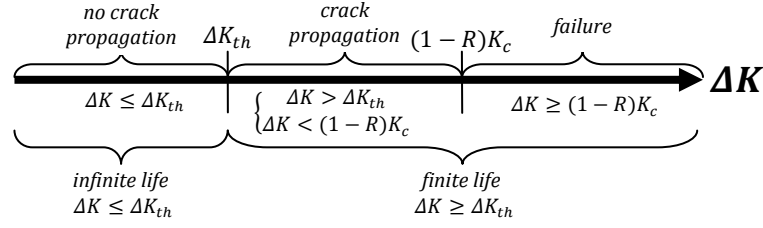


Figure 1: Stress-intensity-factor-range axis representation of hypothesis 5).

According to hypotheses 3) and 5), and with reference to Figure 1, Equation (2) can be further simplified:

$$P[\text{no crack propagation}] = P[\Delta K_{th} \geq \Delta K] = 1 - F_{\Delta K_{th}}[\Delta K]. \quad (3)$$

It can be shown (Appendix A) that, taken hypotheses 1)-5) and Equation (3), the probability of having the logarithm of the crack growth rate, v_a , smaller than a specific value, v_a^* , is given by:

$$F_{v_a}[v_a^*] = 1 - F_{\Delta K_{th}}[\Delta K] + \int_{\frac{\Delta K}{1-R}}^{\overline{K}_c^*} f_{K_c} \left(\int_{\underline{\Delta K}_{th}^*}^{\Delta K} F_{v_a|(\Delta K_{th}, K_c)} f_{\Delta K_{th}} d\Delta K_{th}^* \right) dK_c^*. \quad (4)$$

where $F_{v_a}[v_a^*]$ is the cdf of v_a evaluated at v_a^* , $\underline{\Delta K}_{th}^*$ denotes the lower limit of ΔK_{th} and \overline{K}_c^* represents the upper limit of K_c .

Deriving the right-hand side of Equation (4) with respect to v_a^* , it is possible to obtain the pdf of v_a as follows:

$$f_{v_a}[v_a^*] = \int_{\frac{\Delta K}{1-R}}^{\overline{K}_c^*} f_{K_c} \left(\int_{\underline{\Delta K}_{th}^*}^{\Delta K} f_{v_a|(\Delta K_{th}, K_c)} f_{\Delta K_{th}} d\Delta K_{th}^* \right) dK_c^*, \quad (5)$$

where $f_{v_a}[v_a^*]$ denotes the pdf of v_a evaluated at v_a^* .

2.1. Parameter estimation

The distributions given in Equations (4) and (5) usually depend on a set of r unknown parameters, $\theta = (\theta_1, \theta_2, \dots, \theta_r)$, which must be estimated from the experimental data set through an appropriate estimation method.

Parametric estimation based on the ML Principle is a common practice, since it allows for censoring and truncation of experimental data and it gives raise to estimators with good asymptotic properties (consistency, unbiasedness, efficiency and normality¹⁹).

In the following, the ML Principle is used to estimate the parameters involved in the statistical model given in Equations (4) and (5).

For the statistical model previously defined, with sample data $v_{a_1}^*, v_{a_2}^*, \dots, v_{a_n}^*$, at SIF levels $\Delta K_1, \Delta K_2, \dots, \Delta K_n$, respectively, the Likelihood function, $L[\theta]$, takes the form:

$$L[\theta] = \prod_{i=1}^n f_{v_a}[v_{a_i}^*; \Delta K_i, \theta]. \quad (6)$$

According to the ML Principle, the ML estimate $\tilde{\theta}$ of θ is the set of parameter values that maximizes $L[\theta]$ in Equation (6).

2.2. Number of cycles to failure

A first application based on the proposed statistical model is the estimation of the number of cycles to failure, a quantity often required for reliability prediction of critical components^{20,21}.

Given the initial crack length, a_s , the number of cycles to failure, $N_{f_{a_s}}$, can be computed as follows:

$$N_{f_{a_s}} = \int_{a_s}^{a_c} e^{-v_a} da, \quad (7)$$

where a_c denotes the crack length leading to failure (i.e., the critical crack length).

It can be shown (Appendix B) that, taken Equation (7), the cdf of $N_{f_{a_s}}$, $F_{N_{f_{a_s}}}$, is given by:

$$F_{N_{f_{a_s}}} = 1 - F_{v_a}. \quad (8)$$

Taking into account Equation (8), if the γ -th quantile of $N_{f_{a_s}}$, $N_{f_{a_s},\gamma}$, is of interest, then it can be computed from the $(1 - \gamma)$ -th quantile of v_a , $v_{a,1-\gamma}$, as follows:

$$N_{f_{a_s},\gamma} = \int_{a_s}^{a_{c,\gamma}} e^{-v_{a,1-\gamma}} da, \quad (9)$$

where $a_{c,\gamma}$ is the γ -th quantile of the critical crack length. Indeed, a_c is a monotone decreasing function of v_a (i.e., if $v_{a,1} < v_{a,2}$, then $a_{c,1} > a_{c,2}$) and, as a consequence, if $F_{v_a} = 1 - \gamma$, then $F_{a_c} = \gamma$. In particular, for given ΔK and R , $a_{c,\gamma}$ in Equation (9) can be obtained by solving the following equation:

$$\gamma = F_{K_c} \left[\frac{\Delta K[a_{c,\gamma}]}{1-R} \right],$$

where $\Delta K[a_{c,\gamma}]$ denotes the applied SIF range evaluated at $a_{c,\gamma}$.

2.3. Crack length after a given number of cycles

A second application based on the proposed statistical model is the estimation of the crack length after a given number of cycles, a relevant quantity required for planning inspection intervals of critical components²².

Given the initial crack length, a_s , the crack length after N cycles, $a_{e_{a_s,N}}$, can be computed by solving the following integral:

$$N = \int_{a_s}^{a_{e_{a_s,N}}} e^{-v_a} da. \quad (10)$$

It can be shown (Appendix C) that, taken Equation (10), the cdf of $a_{e_{a_s,N}}$, $F_{a_{e_{a_s,N}}}$, is given by:

$$F_{a_{e_{a_s,N}}} = F_{v_a}. \quad (11)$$

Considering Equation (11), the γ -th quantile of $a_{e_{a_s, N, \gamma}}$, $a_{e_{a_s, N, \gamma}}$, can be computed by solving the following equation:

$$N = \int_{a_s}^{a_{e_{a_s, N, \gamma}}} e^{-v_{a, \gamma}} da, \quad (12)$$

where $v_{a, \gamma}$ is the γ -th quantile of v_a .

3. Numerical example

In the attempt to show potential applications of the proposed statistical approach, a numerical example is discussed hereafter based on the deterministic model adopted in the NASGRO sw v. 4.02⁴. Applicability of the approach goes beyond the illustrated example.

For sake of clarity, the NASGRO model is first rapidly recalled. Secondly, estimation of the parameters necessary to the model is obtained by applying the ML principle to experimental data taken from NASGRO database. Illustrative plots are drawn for statistical prediction of the number of cycles to failure and of the crack length after a given number of cycles.

3.1. NASGRO model

NASGRO model was developed at NASA, based on formulation by Forman and Mettu²³. The crack propagation law is:

$$\frac{da}{dN} = C \left(\frac{1-f}{1-R} \Delta K \right)^n \frac{\left(1 - \frac{\Delta K_{th}}{\Delta K} \right)^p}{\left(1 - \frac{\Delta K}{(1-R)K_C} \right)^q}, \quad (13)$$

where f is the closure function and C , n , p and q are empirical constants.

The dependence of ΔK_{th} on a and R is described by the following equation:

$$\Delta K_{th} = \frac{\Delta K_{th1, \infty}}{\sqrt{1 + \frac{a_0}{a}}} k_1[R] = \frac{\Delta K_{th1, \infty}}{\sqrt{1 + \frac{a_0}{a}}} \begin{cases} \frac{\left(\frac{1-R}{1-f} \right)^{(1+C_{th}^+ R)}}{(1-A_0)^{(1-R)C_{th}^+}}, & R \geq 0 \\ \frac{\left(\frac{1-R}{1-f} \right)^{(1+C_{th}^- R)}}{(1-A_0)^{(C_{th}^+ - C_{th}^- R)}}, & R < 0 \end{cases}, \quad (14)$$

where C_{th}^+ , C_{th}^- and A_0 are constant coefficients, a_0 is the El-Haddad parameter²⁴ and $\Delta K_{th1, \infty}$ denotes the threshold SIF range at $R \rightarrow 1$ and $a \gg a_0$.

The dependence of K_C on specimen thickness, t , can be described by the following equation:

$$K_C = K_{IC} k_2[t] = K_{IC} \left(1 + B_k e^{-\left(A_k \frac{t}{t_0} \right)^2} \right), \quad (15)$$

where K_{IC} is the plane strain fracture toughness, A_k , B_k are constant coefficients, and t_0 is defined as:

$$t_0 = 2500 \left(\frac{K_{Ic}}{S_y} \right)^2, \quad (16)$$

where S_y denotes the material yield strength.

3.2. Parameter estimation and applications

To introduce statistical variability in NASGRO model, the major sources of scatter have to be identified. According to the literature^{1,5,6,13}, it can be assumed that:

- C in Equation (13) belongs to a LogNormal distribution with parameters μ_C and σ_C ;
- n in Equation (13) belongs to a Normal distribution with parameters μ_n and σ_n ;
- $\log[C]$ and n are jointly Normal^{6,25} with correlation coefficient equal to ρ ;
- $\Delta K_{th1,\infty}$ in Equation (14) belongs to a LogNormal distribution with parameters $\mu_{\Delta K_{th1,\infty}}$ and $\sigma_{\Delta K_{th1,\infty}}$;
- K_{Ic} in Equation (15) belongs to a LogNormal distribution with parameters $\mu_{K_{Ic}}$ and $\sigma_{K_{Ic}}$.

The above assumptions are not the only one possible, as the proposed method is open to any choice of distribution types. Alternative statistical distributions can be adopted and their suitability evaluated by carrying out parameter estimation through the Maximum Likelihood Principle and by comparing the obtained Likelihood values.

To ensure fulfillment of hypothesis 5), that is to make sure that the upper limit of the no crack propagation region is below the lower limit of the specimen failure region, distributions of both $\Delta K_{th1,\infty}$ and K_{Ic} have been truncated. Truncation limits are chosen as the best trade-off between the need of providing a sufficiently wide support of the distribution and, on the other side, to cover the widest range possible for the stress ratio R . By truncating the distribution of the logarithm of $\Delta K_{th1,\infty}$ at $\mu_{\Delta K_{th1,\infty}} + 3\sigma_{\Delta K_{th1,\infty}}$ and at $\mu_{K_{Ic}} - 3\sigma_{K_{Ic}}$ the distribution of the logarithm of K_{Ic} , fulfillment of hypothesis 5) is ensured up to R values of 0.96. Symmetric truncation of each distribution is applied so to maintain the symmetry of the distribution. Overall, the probability associated to the truncation of each distribution is very low (equal to 0.3%).

Equation (17) is the statistical pdf adopted for computing the Likelihood function, $L[\boldsymbol{\theta}]$, given in Equation (6). Equation (17) can be obtained from Equation (5) by considering as rv's, $\Delta K_{th1,\infty}$ and K_{Ic} .

$$f_{v_a}[\boldsymbol{\theta}] = \int_{K_{Ic,min}}^{K_{Ic,max}} f_{K_{Ic}} \left(\int_{\Delta K_{th1,\infty,min}}^{\Delta K_{th1,\infty,max}} f_{v_a|(\Delta K_{th1,\infty}, K_{Ic})} f_{\Delta K_{th1,\infty}} d\Delta K_{th1,\infty}^* \right) dK_{Ic}^*, \quad (17)$$

where $\boldsymbol{\theta} = \{\mu_{\Delta K_{th1,\infty}}, \sigma_{\Delta K_{th1,\infty}}, \mu_{K_{Ic}}, \sigma_{K_{Ic}}, \mu_C, \sigma_C, \mu_n, \sigma_n, \rho, p, q\}$, and the pdf's, $f_{v_a|(\Delta K_{th1,\infty}, K_{Ic})}$, $f_{\Delta K_{th1,\infty}}$ and $f_{K_{Ic}}$, and the limits of integration, $\Delta K_{th1,\infty,min}$, $\Delta K_{th1,\infty,max}$, $K_{Ic,min}$ and $K_{Ic,max}$, are listed in Table 1.

Table 1: List of functions and limits of integration used in Equation (17).

$$f_{\Delta K_{th1,\infty}} = \frac{1}{\Delta K_{th1,\infty}^* \sigma_{\Delta K_{th1,\infty}}} \frac{\phi \left[\frac{\log[\Delta K_{th1,\infty}^*] - \mu_{\Delta K_{th1,\infty}}}{\sigma_{\Delta K_{th1,\infty}}} \right]}{2\Phi[3] - 1}$$

$$\begin{cases} \Delta K_{th1,\infty,min} = e^{\mu_{\Delta K_{th1,\infty}} - 3\sigma_{\Delta K_{th1,\infty}}} \\ \Delta K_{th1,\infty,max} = \min[\max[e^{\mu_{\Delta K_{th1,\infty}} - 3\sigma_{\Delta K_{th1,\infty}}}, \Delta K/k_1[0]], e^{\mu_{\Delta K_{th1,\infty}} + 3\sigma_{\Delta K_{th1,\infty}}}] \end{cases}$$

$$f_{K_{Ic}} = \frac{1}{K_{Ic}^* \sigma_{K_{Ic}}} \frac{\phi \left[\frac{\log[K_{Ic}^*] - \mu_{K_{Ic}}}{\sigma_{K_{Ic}}} \right]}{2\Phi[3] - 1}$$

$$\begin{cases} K_{Ic,min} = \min[\max[e^{\mu_{K_{Ic}} - 3\sigma_{K_{Ic}}}, \Delta K/k_2[3.048]], e^{\mu_{K_{Ic}} + 3\sigma_{K_{Ic}}}] \\ K_{Ic,max} = e^{\mu_{K_{Ic}} + 3\sigma_{K_{Ic}}} \end{cases}$$

$$f_{v_a | (\Delta K_{th1,\infty}, K_{Ic})} = \frac{1}{\sigma_{v_a}} \phi \left[\frac{v_a^* - \mu_{v_a}}{\sigma_{v_a}} \right]$$

$$\begin{cases} \mu_{v_a} = \mu_C + \mu_n \cdot \log[(1-f) \cdot \Delta K] + p \cdot \log \left[1 - \frac{k_1[0]}{\sqrt{1 + \frac{a_0}{a}}} \frac{\Delta K_{th1,\infty}^*}{\Delta K} \right] - q \cdot \log \left[1 - \frac{1}{k_2[3.048]} \frac{\Delta K}{K_{Ic}^*} \right] \\ \sigma_{v_a} = \sqrt{\sigma_C^2 + \sigma_n^2 (\log[(1-f) \cdot \Delta K])^2 + 2\rho\sigma_C\sigma_n \log[(1-f) \cdot \Delta K]} \end{cases}$$

Note: $\phi[\cdot]$ and $\Phi[\cdot]$ denote the standardized Normal pdf and cdf, respectively. $f_{v_a | (\Delta K_{th1,\infty}, K_{Ic})}$ has been obtained by considering that $v_a | (\Delta K_{th1,\infty}, K_{Ic}) = \log[C] + n \cdot \log[(1-f) \cdot \Delta K] + constant$, where $\log[C]$ and n are jointly Normal with correlation coefficient ρ .

To ensure conservative predictions²⁵ and for sake of simplicity, σ_n is assumed equal to 0 and, consequently, n is considered a parameter to be estimated. With this assumption, σ_{v_a} becomes equal to σ_C , regardless of the value of the correlation coefficient ρ . Nevertheless, it is worth noting that the assumption of σ_n equal to 0 can be relaxed, since σ_n and ρ can be treated as parameters to be estimated, obviously at the price of increased computational complexity.

Coefficients f , $k_1[0]$, a_0 and $k_2[3.048]$, which appear in Table 1, can be computed through functions and coefficient values listed in Table 2. Both functions and coefficients are taken from NASGRO database and refer to an AISI 4340 steel plate, 3.048 mm in thickness, tested at $R = 0$ (ref. C4DI13AB1 in NASGRO sw v. 4.02⁴).

Table 2: NASGRO functions and coefficients.

| NASGRO functions | NASGRO coefficients |
|--|---|
| $\sqrt{1 + \frac{a_0}{a}} \cong 1$ | $\begin{cases} a_0 = 0.038 \text{ mm} \\ a \gg a_0 \end{cases}$ |
| $A_0 = (0.825 - 0.34\alpha + 0.05\alpha^2) \sqrt[3]{\cos[\pi\rho_S/2]} = 0.275$ | $\begin{cases} \alpha = 2.5 \\ \rho_S = 0.3 \end{cases}$ |
| $f = \max[0, A_0] = 0.275$ | - |
| $k_1[0] = (1 - f)^{-1}(1 - A_0)^{-C_{th}^+} = 1.378$ | $C_{th}^+ = 0$ |
| $\begin{cases} t_0 = 2500(E[K_{Ic}]/S_y)^2 = 0.032^2 e^{2\mu_{K_{Ic}} + \sigma_{K_{Ic}}^2} \\ k_2[3.048] = 1 + B_k e^{-(A_k \frac{3.048}{t_0})^2} = 1 + 0.5 e^{-2300^2 e^{-2(2\mu_{K_{Ic}} + \sigma_{K_{Ic}}^2)}} \end{cases}$ | $\begin{cases} S_y = 1586 \text{ MPa} \\ A_k = 0.75 \\ B_k = 0.5 \end{cases}$ |

Note: t_0 has been computed by substituting the expectation of K_{Ic} , $E[K_{Ic}] = e^{\mu_{K_{Ic}} + \sigma_{K_{Ic}}^2/2}$, to K_{Ic} in Equation (16).

Parameter estimates are obtained by applying the ML principle to material data taken from NASGRO database. The vector of estimates, obtained through a maximization code implemented in MATLAB®, is found to be:

$$\begin{aligned} \tilde{\theta} &= \{\tilde{\mu}_{\Delta K_{th1,\infty}}, \tilde{\sigma}_{\Delta K_{th1,\infty}}, \tilde{\mu}_{K_{Ic}}, \tilde{\sigma}_{K_{Ic}}, \tilde{\mu}_C, \tilde{\sigma}_C, \tilde{\mu}_n, \tilde{p}, \tilde{q}\} = \\ &= \{1.037, 0.161, 4.574, 0.174, -20.92, 0.166, 1.668, 2.549, 0.861\}, \end{aligned}$$

where the tilde accent mark, $\tilde{\cdot}$, denotes estimated values.

In order to plot crack growth rate functions for different probability values, it is still necessary to define the estimated statistical cdf of v_a , $\tilde{F}_{v_a}[v_a^*, \Delta K]$. Starting from Equation (4), $\tilde{F}_{v_a}[v_a^*, \Delta K]$ can be obtained by considering as rv's, $\Delta K_{th1,\infty}$ and K_{Ic} , and by substituting the true functions with the estimated functions:

$$\begin{aligned} \tilde{F}_{v_a}[v_a^*, \Delta K] &= 1 - \tilde{F}_{\Delta K_{th}}[\Delta K] + \\ &+ \int_{\tilde{K}_{Ic,min}}^{\tilde{K}_{Ic,max}} \tilde{f}_{K_{Ic}} \left(\int_{\tilde{\Delta K}_{th1,\infty,min}}^{\tilde{\Delta K}_{th1,\infty,max}} \tilde{F}_{v_a|(\Delta K_{th1,\infty}, K_{Ic})} \cdot \tilde{f}_{\Delta K_{th1,\infty}} d\Delta K_{th1,\infty}^* \right) dK_{Ic}^*. \quad (18) \end{aligned}$$

In Equation (18), the estimated pdf's $\tilde{f}_{\Delta K_{th1,\infty}}$ and $\tilde{f}_{K_{Ic}}$, and the estimated limits of integration, $\tilde{\Delta K}_{th1,\infty,min}$, $\tilde{\Delta K}_{th1,\infty,max}$, $\tilde{K}_{Ic,min}$ and $\tilde{K}_{Ic,max}$, can easily be obtained by substituting $\tilde{\theta}$ to θ in Tables 1 and 2; in addition, the estimated cdf's, $\tilde{F}_{\Delta K_{th}}[\Delta K]$ and $\tilde{F}_{v_a|(\Delta K_{th1,\infty}, K_{Ic})}$, are respectively equal to:

$$\tilde{F}_{\Delta K_{th}}[\Delta K] = \frac{\Phi \left[\frac{\log[\Delta K/k_1[0]] - \tilde{\mu}_{\Delta K_{th1,\infty}}}{\tilde{\sigma}_{\Delta K_{th1,\infty}}} \right] + \Phi[3] - 1}{2\Phi[3] - 1}$$

and

$$\tilde{F}_{v_a|(\Delta K_{th1,\infty}, K_{Ic})} = \Phi \left[\frac{v_a^* - \tilde{\mu}_{v_a}}{\tilde{\sigma}_{v_a}} \right].$$

Figure 2 shows estimated crack growth rate functions for different probability values, γ . For each γ , the sigmoidal curve is obtained by solving $\tilde{F}_{v_a}[\tilde{v}_{a,\gamma}^*, \Delta K] = \gamma$ with respect to $\tilde{v}_{a,\gamma}^*$, for different ΔK values. As it can be observed, probabilistic curves conform well to experimental data. Furthermore, the model well represents the well-known larger data scatter in the near-threshold and unstable crack propagation regions.

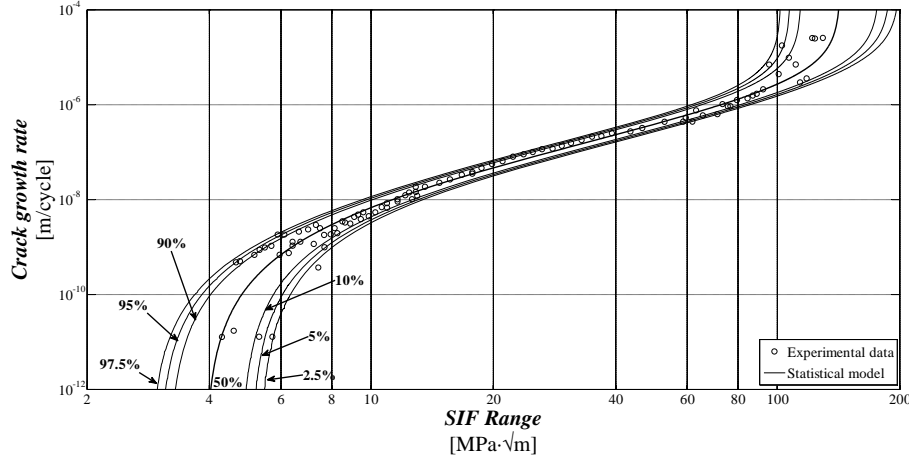


Figure 2: Plots of crack growth rate functions obtained with the proposed statistical distribution at different probability values. Experimental data points are taken from material NASGRO database⁴.

Once the γ -th quantile curve of v_a is estimated, the $(1 - \gamma)$ -th quantile of the number of cycles to failure can be obtained through Equation (9). In Equation (9), integration with respect to a is possible after having expressed the SIF range ΔK as a function of the stress range, $\Delta\sigma$:

$$\Delta K = Y[a] \cdot \Delta\sigma \cdot \sqrt{\pi \cdot a}.$$

where $Y[a]$ is the geometry correction factor.

Similarly, probabilistic curves of the crack length after a given number of cycles can be obtained through Equation (12).

The illustrative plots of Figure 3 and 4 are drawn for the case of a center-through crack in a tensile 100x10 mm plate. For a center-through crack of finite width plate, the geometry correction factor can be expressed as:

$$Y[a] = \sqrt{\secant\left[\pi \frac{a}{w}\right]},$$

where $2a$ is the crack length and w is the plate width.

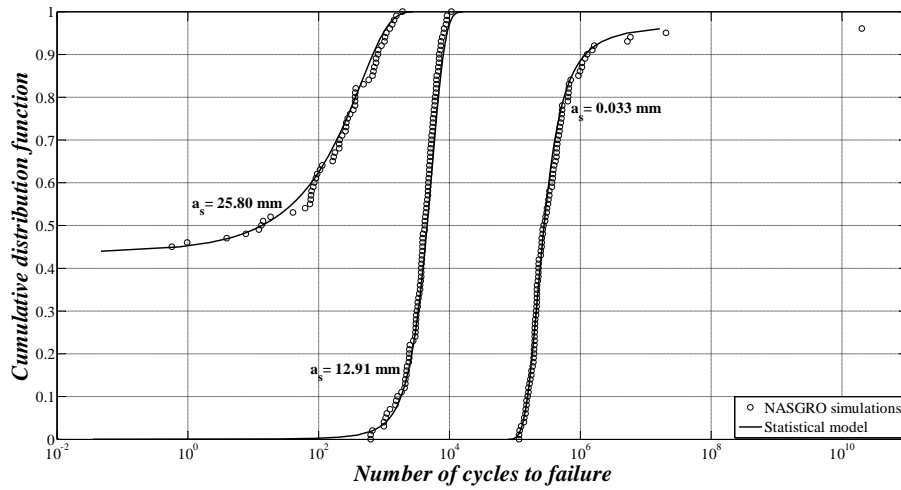


Figure 3: Number of cycles to failure for different initial crack lengths: comparison between simulated (empty circles) and proposed analytical cumulative distribution functions (black lines). $\Delta\sigma = 350$ MPa at $R = 0$.

The data denoted as “NASGRO simulations” in the legend, that appear in Figures 3 and 4, were obtained by running one hundred NASGRO computations. The required input material parameters, $\Delta K_{th1,\infty}$, K_{Ic} and C , were randomly drawn (Monte Carlo simulations) from the estimated distributions; the other parameters, n , p and q , were taken from the vector of estimates $\tilde{\theta}$. As in the case of Figure 2, the proposed statistical model well compares with NASGRO results.

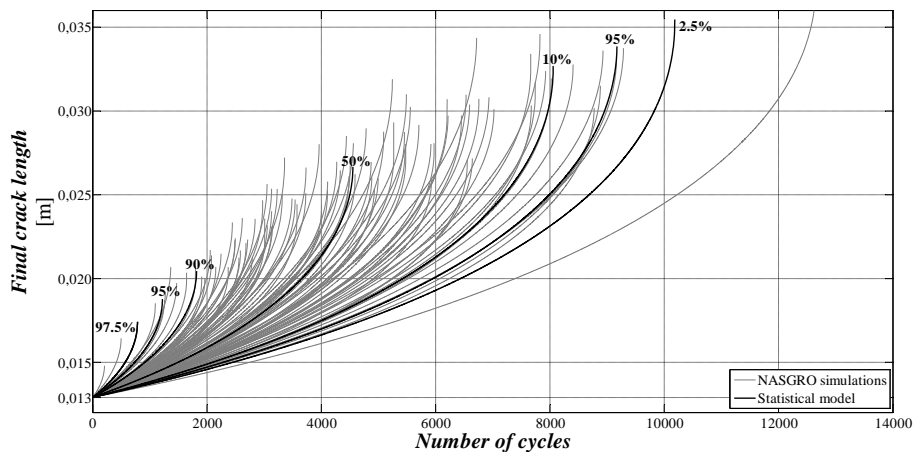


Figure 4: Final crack length after different number of cycles: proposed analytical curves at different probability values (black lines) as they compare with 100 NASGRO simulations (grey lines). $\Delta\sigma = 350$ MPa at $R = 0$; $a_s = 12.91$ mm.

It should be noted that probabilistic curves plotted in Figure 2 are obtained by computing exact confidence intervals for v_a at different ΔK values (point-wise confidence bands). In this respect, they only approximate the exact confidence bands for the curve of v_a as a function of ΔK (simultaneous confidence bands). Indeed, it is well known in the literature²⁶ that, even if commonly adopted for estimating probabilistic curves, point-wise confidence bands do not generally coincide with simultaneous confidence bands and can only provide approximated

results. Consequently, if point-wise confidence bands are considered for computing the number of cycles to failure or the crack length after a given number of cycles, the computed values only approximate the exact results. Nevertheless, approximation is generally negligible, as shown in Figures 3 and 4.

4. Conclusions

A statistical distribution for the sigmoidal crack growth rate function is introduced. Due to the general nature of the proposed distribution, any deterministic sigmoidal crack propagation model can be utilized.

For obtaining material estimates, the ML Principle is adopted. No distinction among the three regions of crack propagation is considered: all data points were taken into account as belonging to the same population.

Reliability predictions (i.e., the number of cycles to failure and the crack length after a given number of cycles) are obtained through numerical integration of analytical functions with no need of Monte Carlo simulations.

Effectiveness of the proposed statistical model is shown through examples based on NASGRO algorithm.

Further research is in progress to extend the applicability of the developed statistical distribution to the case of variable amplitude loading, including load-interaction effects (e.g., Wheeler and Willenborg load-interaction models).

APPENDIX A

Cumulative distribution function of v_a

Taken hypotheses 1)-5) in Section 2, the probability of having, in the stable crack propagation region (Figure 1), v_a smaller than v_a^* is given by:

$$P \left[v_a \leq v_a^*, \Delta K_{th} < \Delta K, K_c > \frac{\Delta K}{(1-R)} \right] = \int_{\frac{\Delta K}{1-R}}^{\overline{K_c^*}} f_{K_c} [K_c^*] \left(\int_{\underline{\Delta K_{th}^*}}^{\Delta K} F_{v_a | (\Delta K_{th}, K_c)} [v_a^*; \Delta K_{th}^*, K_c^*] f_{\Delta K_{th}} [\Delta K_{th}^*] d\Delta K_{th}^* \right) dK_c^*. \quad (A.1)$$

Whereas the events $\Delta K \leq \Delta K_{th}$, $\Delta K_{th} < \Delta K < K_c(1-R)$ and $\Delta K \geq K_c(1-R)$ form a partition of the whole sample space (Figure 1), it follows that the probability of the event $v_a \leq v_a^*$ is given by:

$$P[v_a \leq v_a^*] = P[v_a \leq v_a^* | \Delta K_{th} \geq \Delta K] P[\Delta K_{th} \geq \Delta K] + P \left[v_a \leq v_a^*, \Delta K_{th} < \Delta K, K_c > \frac{\Delta K}{(1-R)} \right] + P \left[v_a \leq v_a^* | K_c \leq \frac{\Delta K}{1-R} \right] P \left[K_c \leq \frac{\Delta K}{1-R} \right]. \quad (A.2)$$

Since v_a approaches $-\infty$ (i.e., the crack growth rate is equal to 0 in the no crack propagation region) when $\Delta K_{th} \geq \Delta K$, then $P[v_a \leq v_a^* | \Delta K_{th} \geq \Delta K] = 1$; moreover, since v_a approaches $+\infty$ (i.e., the crack growth rate is infinite when failure occurs) when $K_c \leq \frac{\Delta K}{1-R}$, then

$P \left[v_a \leq v_a^* | K_c \leq \frac{\Delta K}{1-R} \right] = 0$. Therefore, Equation (A.2) simplifies as follows:

$$P[v_a \leq v_a^*] = P[\Delta K_{th} \geq \Delta K] + P \left[v_a \leq v_a^*, \Delta K_{th} < \Delta K, K_c > \frac{\Delta K}{(1-R)} \right]. \quad (A.3)$$

Taking into account Equations (3) and (A.1), Equation (A.3) finally yields:

$$F_{v_a} [v_a^*] = 1 - F_{\Delta K_{th}} [\Delta K] + \int_{\frac{\Delta K}{1-R}}^{\overline{K_c^*}} f_{K_c} [K_c^*] \left(\int_{\underline{\Delta K_{th}^*}}^{\Delta K} F_{v_a | (\Delta K_{th}, K_c)} [v_a^*; \Delta K_{th}^*, K_c^*] f_{\Delta K_{th}} [d\Delta K_{th}^*] \right) dK_c^*.$$

APPENDIX B

Cumulative distribution function of $N_{f_{a_s}}$

Consider two different crack growth rate functions, whose logarithms are denoted as $v_{a,1}$ and $v_{a,2}$. Suppose that $v_{a,1}$ is defined in the range $(a_{th,1}, a_{c,1})$, where $a_{th,1}$ denotes the threshold crack length of $v_{a,1}$ (crack length value for which $v_{a,1} = -\infty$) and $a_{c,1}$ is the critical crack length of $v_{a,1}$ (crack length value for which $v_{a,1} = +\infty$). Analogously, suppose that $v_{a,2}$ is defined in the range $(a_{th,2}, a_{c,2})$, where $a_{th,2}$ denotes the threshold crack length of $v_{a,2}$ (crack length value for which $v_{a,2} = -\infty$) and $a_{c,2}$ is the critical crack length of $v_{a,2}$ (crack length value for which $v_{a,2} = +\infty$). Furthermore, suppose that $v_{a,1} < v_{a,2}$. Being the logarithm of the crack growth rate a monotone increasing function ranging from $-\infty$ to $+\infty$, then $a_{th,2} < a_{th,1}$ and $a_{c,2} < a_{c,1}$.

Suppose that $a_{th,2} < a_{th,1} < a_s < a_{c,2} < a_{c,1}$, then Equation (7) becomes:

$$N_{f_{a_s,1}} = \int_{a_s}^{a_{c,1}} e^{-v_{a,1}} da, \quad (\text{B.1})$$

when $v_{a,1}$ is considered, and

$$N_{f_{a_s,2}} = \int_{a_s}^{a_{c,2}} e^{-v_{a,2}} da, \quad (\text{B.2})$$

when $v_{a,2}$ is considered.

The domain of integration of Equation (B.2) can be extended up to $a_{c,1}$, since $e^{-v_{a,2}} \equiv 0$ in the range $[a_{c,2}, a_{c,1}]$:

$$N_{f_{a_s,2}} = \int_{a_s}^{a_{c,2}} e^{-v_{a,2}} da + \int_{a_{c,2}}^{a_{c,1}} 0 da = \int_{a_s}^{a_{c,1}} e^{-v_{a,2}} da. \quad (\text{B.3})$$

Taking into account Equations (B.1) and (B.3) and considering that $v_{a,1} < v_{a,2}$ and, consequently, $e^{-v_{a,1}} > e^{-v_{a,2}}$, it follows that $N_{f_{a_s,1}} > N_{f_{a_s,2}}$. Therefore, according to Equation (7), $N_{f_{a_s}}$ is a monotone decreasing function of v_a .

According to Theorem 2.1.3 in²⁷, if $a_{th} < a_s < a_c$, the complementary cdf of $N_{f_{a_s}}$ is finally given by:

$$1 - F_{N_{f_{a_s}}|a_{th} < a_s < a_c} = F_{v_a|a_{th} < a_s < a_c}, \quad (\text{B.4})$$

where $F_{N_{f_{a_s}}|a_{th} < a_s < a_c}$ is the conditional cdf of $N_{f_{a_s}}$ given that $a_{th} < a_s < a_c$, and $F_{v_a|a_{th} < a_s < a_c}$ denotes the conditional cdf of v_a given that $a_{th} < a_s < a_c$.

Taking Equation (7), if $a_s \geq a_c$, then $N_{f_{a_s}} = 0$ and, as a consequence:

$$1 - F_{N_{f_{a_s}}|a_s \geq a_c} = P[0 > N_{f_{a_s}}^*] = 0, \quad (\text{B.5})$$

where $F_{N_{f_{a_s}}|a_s \geq a_c}$ is the conditional cdf of $N_{f_{a_s}}$ given that $a_s \geq a_c$.

Finally, if $a_s \leq a_{th}$, then $N_{f_{a_s}} \rightarrow +\infty$ and, as a consequence:

$$1 - F_{N_{f_{a_s}}|a_s \leq a_{th}} = P[+\infty > N_{f_{a_s}}^*] = 1. \quad (\text{B.6})$$

where $F_{N_{f_{a_s}}|a_s \leq a_{th}}$ is the conditional cdf of $N_{f_{a_s}}$ given that $a_s \leq a_{th}$.

Provided that the events $a_s \leq a_{th}$, $a_{th} < a_s < a_c$ and $a_s \geq a_c$ form a partition of the whole sample space, it follows, from Equations (B.4)-(B.6) that the complementary cdf of $N_{f_{a_s}}$ is given by:

$$1 - F_{N_{f_{a_s}}} = P[a_{th} \geq a_s] + F_{v_a|a_{th} < a_s < a_c} P[a_{th} < a_s < a_c]. \quad (\text{B.7})$$

Since the SIF range is a monotone increasing function of the crack length, then a_{th} , a_c and a_s in Equation (B.7) can be substituted by ΔK_{th} , $K_c(1 - R)$ and ΔK (a_s can be any a value below a_c), thus giving:

$$1 - F_{N_{f_{a_s}}} = P[\Delta K_{th} \geq \Delta K] + P[v_a \leq v_a^*, \Delta K_{th} < \Delta K < K_c(1 - R)]. \quad (B.8)$$

Taken (Equation A.3):

$$P[v_a \leq v_a^*] = P[\Delta K_{th} \geq \Delta K] + P\left[v_a \leq v_a^*, \Delta K_{th} < \Delta K, K_c > \frac{\Delta K}{(1-R)}\right],$$

equation (B.8) finally yields:

$$1 - F_{N_{f_{a_s}}} = P[v_a \leq v_a^*] = F_{v_a},$$

or, equivalently:

$$F_{N_{f_{a_s}}} = 1 - F_{v_a}.$$

APPENDIX C

Cumulative distribution function of $a_{e_{a_s, N}}$

Consider the two functions $v_{a,1}$ and $v_{a,2}$ introduced in Appendix B: i.e., $v_{a,1}$ defined in the range $(a_{th,1}, a_{c,1})$, $v_{a,2}$ defined in the range $(a_{th,2}, a_{c,2})$, being $v_{a,1} < v_{a,2}$.

Suppose that $a_{th,2} < a_{th,1} < a_s < a_{c,2} < a_{c,1}$. For a given N , since the integrand in Equation (10) is a positive-definite function, if $v_{a,1} < v_{a,2}$ (i.e., $e^{-v_{a,1}} > e^{-v_{a,2}}$), then there must exist two different $a_{e_{a_s, N}}$ values, $a_{e_{a_s, N}, 1}$ and $a_{e_{a_s, N}, 2}$, such that:

$$N = \int_{a_s}^{a_{e_{a_s, N}, 1}} e^{-v_{a,1}} da, \quad (C.1)$$

when $v_{a,1}$ is considered, and

$$N = \int_{a_s}^{a_{e_{a_s, N}, 2}} e^{-v_{a,2}} da, \quad (C.2)$$

when $v_{a,2}$ is considered. It is worth noting that the given value of N is upper limited to $N_{f_{a_s}}$; this follows from considering that the integral function in Equation (10) reaches the value $N_{f_{a_s}}$ when $a_{e_{a_s, N}} = a_c$, and remains equal to $N_{f_{a_s}}$ in the open range $[a_c, +\infty)$.

According to Equation (10), N represents the area enclosed by function e^{-v_a} , in the range $[a_s, a_{e_{a_s, N}}]$, and the a -axis: therefore, taking into account Equations (C.1) and (C.2), in order to maintain the area constant, if $e^{-v_{a,1}} > e^{-v_{a,2}}$, then it must be $a_{e_{a_s, N}, 1} < a_{e_{a_s, N}, 2}$. Therefore, $a_{e_{a_s, N}}$ is a monotone increasing function of v_a and, according to Theorem 2.1.3 in²⁷, if $a_{th} < a_s < a_c$, a conditional cdf of $a_{e_{a_s, N}}$, is finally given by:

$$F_{a_{e_{a_s, N}} | a_{th} < a_s < a_c} = F_{v_a | a_{th} < a_s < a_c}, \quad (C.3)$$

where $F_{a_{e_{a_s, N}} | a_{th} < a_s < a_c}$ is the conditional cdf of $a_{e_{a_s, N}}$ given that $a_{th} < a_s < a_c$.

Taken Equation (10), if $a_s \geq a_c$, then $a_{e_{a_s,N}} \rightarrow +\infty$ regardless of the value of N and, as a consequence:

$$F_{a_{e_{a_s,N}}|a_s \geq a_c} = P\left[+\infty \leq a_{e_{a_s,N}}^*\right] = 0, \quad (C.4)$$

where $F_{a_{e_{a_s,N}}|a_s \geq a_c}$ is the conditional cdf of $a_{e_{a_s,N}}$ given that $a_s \geq a_c$.

Finally, if $a_s \leq a_{th}$, then $a_{e_{a_s,N}} = a_s$ regardless of the value of N and, as a consequence:

$$F_{a_{e_{a_s,N}}|a_s \leq a_{th}} = P\left[a_s \leq a_{e_{a_s,N}}^*\right] = 1. \quad (C.5)$$

where $F_{a_{e_{a_s,N}}|a_s \leq a_{th}}$ is the conditional cdf of $a_{e_{a_s,N}}$ given that $a_s \leq a_{th}$.

Provided that the events $a_s \leq a_{th}$, $a_{th} < a_s < a_c$ and $a_s \geq a_c$ form a partition of the whole sample space, it follows, from Equations (C.3)-(C.5) that the cdf of $a_{e_{a_s,N}}$ is given by:

$$F_{a_{e_{a_s,N}}} = P[a_{th} \geq a_s] + F_{v_a|a_{th} < a_s < a_c} P[a_{th} < a_s < a_c]. \quad (C.6)$$

Since the SIF range is a monotone increasing function of the crack length, then a_{th} , a_c and a_s in Equation (C.6) can be substituted by ΔK_{th} , $K_c(1 - R)$ and ΔK (a_s can be any a value below a_c), thus giving:

$$F_{a_{e_{a_s,N}}} = P[\Delta K_{th} \geq \Delta K] + P[v_a \leq v_a^*, \Delta K_{th} < \Delta K < K_c(1 - R)]. \quad (C.7)$$

Taken (Equation A.3):

$$P[v_a \leq v_a^*] = P[\Delta K_{th} \geq \Delta K] + P\left[v_a \leq v_a^*, \Delta K_{th} < \Delta K, K_c > \frac{\Delta K}{(1-R)}\right],$$

equation (C.7) finally yields:

$$F_{a_{e_{a_s,N}}} = P[v_a \leq v_a^*] = F_{v_a}.$$

References

- 1 Li, W., Sakai, T., Li, Q. and Wang, P. (2011) Statistical analysis of fatigue crack growth behavior for grade B cast steel. *Mater. Des.* **32**, 1262-1272.
- 2 Collipriest, J.E., Ehret, R.M. and Thatcher, C. (1973) *Fracture mechanics equation for cyclic growth*. NASA Technology Utilization Report, MFS-24447.
- 3 Anderson, T.L. (1995) *Fracture mechanics: fundamentals and applications*. 2nd Edition, CRC Press, Boca Raton, USA.
- 4 NASGRO (2002) *Fracture Mechanics and Fatigue Crack Growth Analysis Software. Reference Manual. Version 4.02*. South Research Institute, San Antonio, TX, USA.
- 5 Beretta, S. and Carboni, M. (2006) Experiments and stochastic model for propagation lifetime of railway axles. *Engng. Fract. Mech.* **73**, 2627-2641.
- 6 Beretta, S. and Villa, A. (2008) A rv approach for the analysis of fatigue crack growth with NASGRO equation. *4th International ASRANet Colloquium*, 25-27 June 2008, Athens, Greece.
- 7 Al-Rubaie, K.S., Barroso, E.K.L. and Godefroid, L.B. (2008) Statistical modeling of fatigue crack growth rate in pre-strained 7475-T7351 aluminum alloy. *Mater. Sci. Engng. A* **486**, 585-595.
- 8 Provan, J.W. (1987) *Probabilistic fracture mechanics and reliability*. Martinus Nijhoff Publishers, Dordrecht, Netherlands.
- 9 Maymon, G. (1996) The problematic nature of the application of stochastic crack growth models in engineering design. *Engng. Fract. Mech.* **53**, 911-916.
- 10 Cross, R.J., Makeev, A. and Armanios, E. (2006) A comparison of predictions from probabilistic crack growth models inferred from Virkler's data. *J. ASTM Int.* **3**, 1-11.
- 11 Yang, J.N. and Manning, S.D. (1996) A simple second order approximation for stochastic crack growth analysis. *Engng. Fract. Mech.* **53**, 677-686.
- 12 Wu, W.F. and Ni, C.C. (2003) A study of stochastic fatigue crack growth modeling through experimental data. *Probab. Engng. Mech.* **18**, 107-118.
- 13 Ahn, J.J. and Ochiai, S. (2003) Statistical analysis for application of the Paris equation to whisker reinforced metal matrix composites. *Int. J. Fatigue* **25**, 231-236.
- 14 Shen, W., Soboyejo, A.B.O. and Soboyejo, W.O. (2001) Probabilistic modeling of fatigue crack growth in Ti-6Al-4V. *Int. J. Fatigue* **23**, 917-925.
- 15 Rabinowicz, Y., Roman, I. and Ritov, Y. (2008) Advanced methodology for assessing distribution characteristics of Paris equation coefficients to improve fatigue life prediction. *Fatigue Fract. Engng. Mater. Struct.* **31**, 262-269.

- 16 Hariharan, K. and Prakash, R.V. (2011) A study of multi-segment fatigue crack growth data analysis procedure for probabilistic crack growth prediction. *Int. J. Fatigue* **33**, 1557-1563.
- 17 Liu, Y. and Mahadevan, S. (2009) Probabilistic fatigue life prediction using an equivalent initial flaw size distribution. *Int. J. Fatigue* **31**, 476-487.
- 18 Xiang, Y., Lu, Z. and Liu, Y. (2010) Crack growth-based fatigue life prediction using an equivalent initial flaw model. Part I: uniaxial loading. *Int. J. Fatigue* **32**, 341-349.
- 19 Bain, L. J. and Engelhardt, M. (1991) *Statistical Analysis of Reliability and Life-Testing Models: Theory and Methods*. 2nd Edition, Dekker, New York, USA.
- 20 Citarella, R. and Apicella, A. (2006) Advanced design concepts and maintenance by integrated risk evaluation for aerostructures. *Struct. Durab. Health Monitor.* **2**, 183-196.
- 21 Chen, F., Wang, F. and Cui, W. (2011) Fatigue life prediction of engineering structures subjected to variable amplitude loading using the improved crack growth rate model. *Fatigue Fract. Engng. Mater. Struct.* **35**, 278-290.
- 22 Müller, C. H., Gunkel, C. and Denecke, L. (2011) Statistical analysis of damage evolution with a new image tool. *Fatigue Fract. Engng. Mater. Struct.* **34**, 510-520.
- 23 Forman, R.G. and Mettu, S.R. (1992) Behavior of surface and corner cracks subjected to tensile and bending loads in Ti-6Al-4V alloy. *ASTM STP* **1131**, 519-546.
- 24 El-Haddad, M.H., Smith, K.N. and Topper, T.H. (1979) Fatigue crack propagation of short crack. *J. Eng. Mater. Tech.* **101**, 42-46.
- 25 Annis, C. (2003) Probabilistic life prediction isn't as easy as it looks. *ASTM STP* **1450**, 1-13.
- 26 Klein, J.P. and Moeschberger, M.L. (2003) *Survival Analysis: Techniques for Censored and Truncated Data*. Springer, New York, USA.
- 27 Casella, G. and Berger, R.L. (2002) *Statistical inference*. Duxbury, Pacific Grove, USA.